

Facile synthesis of cationic covalent organic frameworks with abundant protonated pyridine nitrogen groups for selective absorption of organic dyes

Shuanglong Lu*, Kunpeng Zhang, Yu Wu, Fang Duan, Mingliang Du

Key Laboratory of Synthetic and Biological Colloids, Ministry of Education, School of Chemical and Material Engineering, Jiangnan University, Wuxi, Jiangsu 214122, P. R. China.

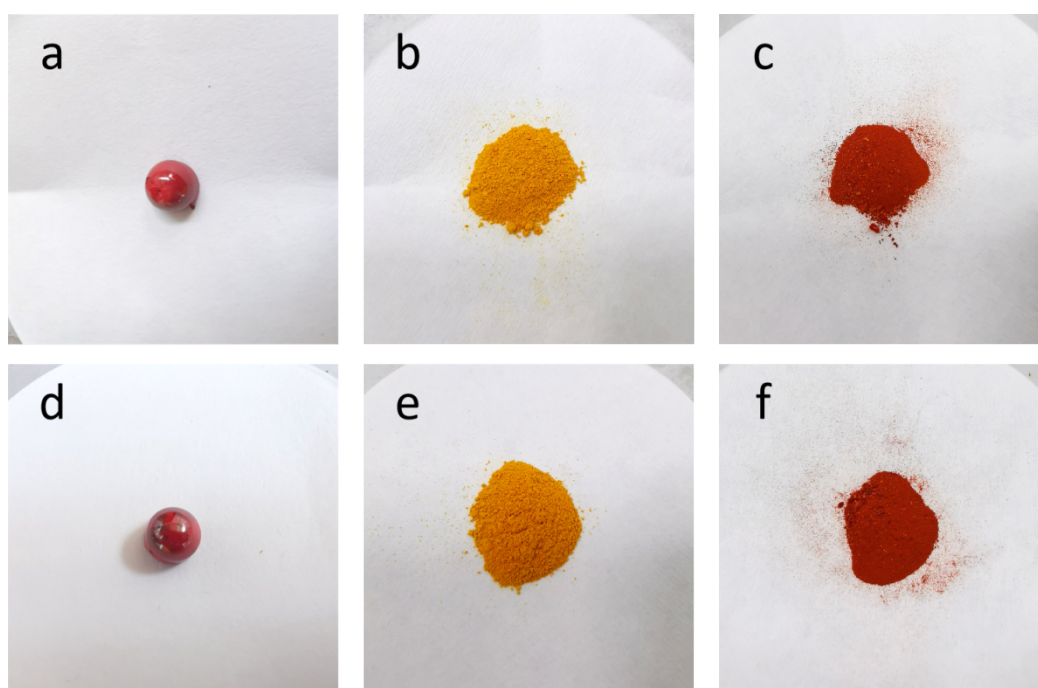


Fig. S1 Pictures of crude product for S (a), S-COF (b), S-iCOF (c), crude product for L (d), L-COF (e) and L-iCOF (f).

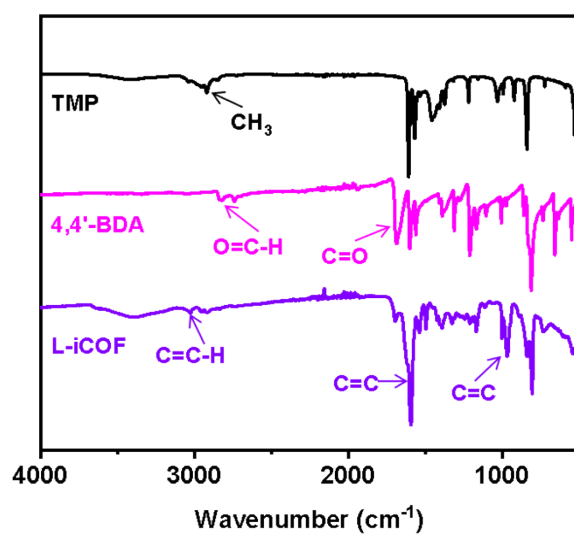


Fig. S2 FT-IR spectra of L-iCOF and corresponding monomers.

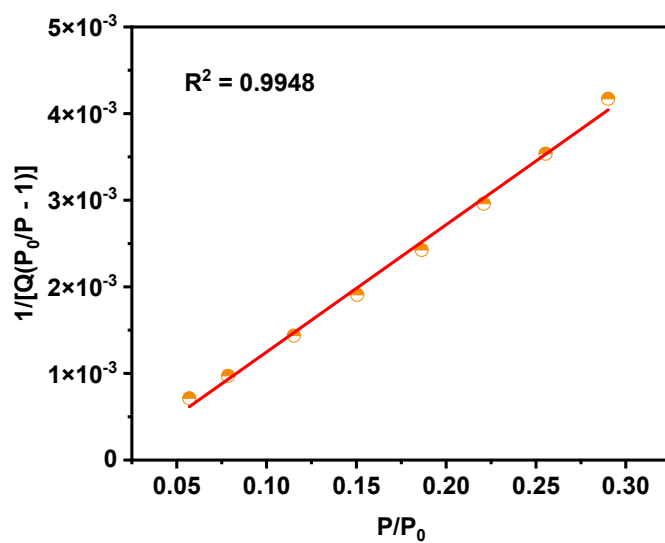


Fig. S3 BET surface area plot calculated from isotherms of S-iCOF ($R^2 = 0.9948$).

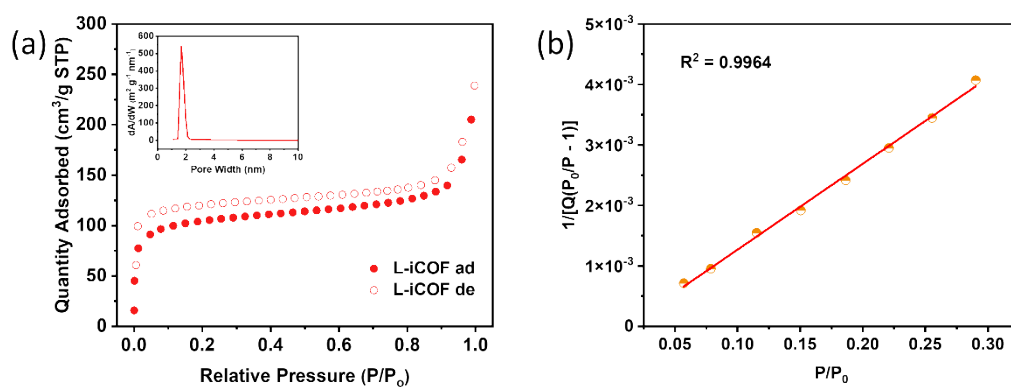


Fig. S4 (a) N_2 adsorption-desorption isotherms of L-iCOF at 77 K. Inset: pore distribution calculated by quenched solid density functional theory. (b) BET surface area plot calculated from isotherms of L-iCOF ($R^2=0.9964$).

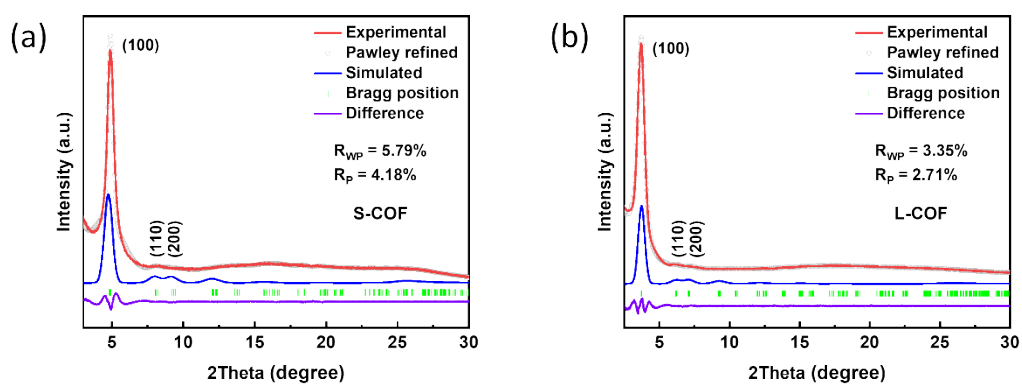


Fig. S5 PXRD patterns of (a) S-COF and (b) L-COF.

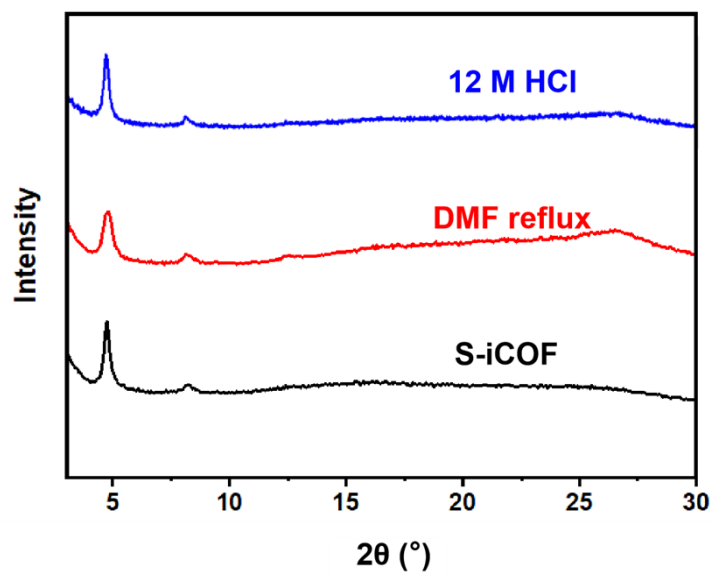


Fig. S6 PXR D patterns of S-iCOF after soaking in concentrated acid and boiling DMF.

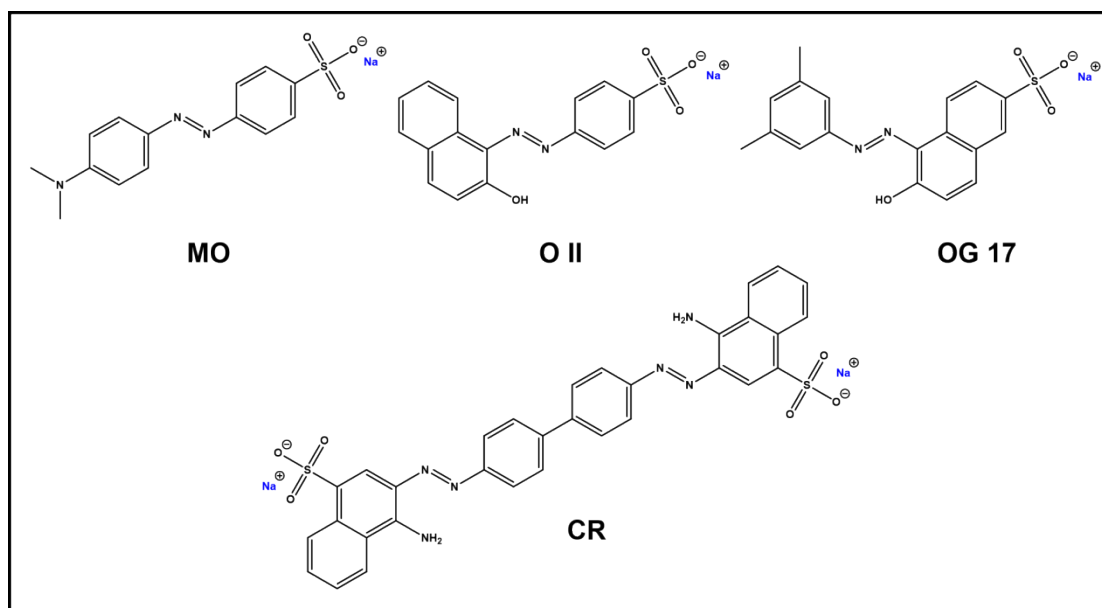


Fig. S7 Molecular structures of anionic organic dyes used in this work.

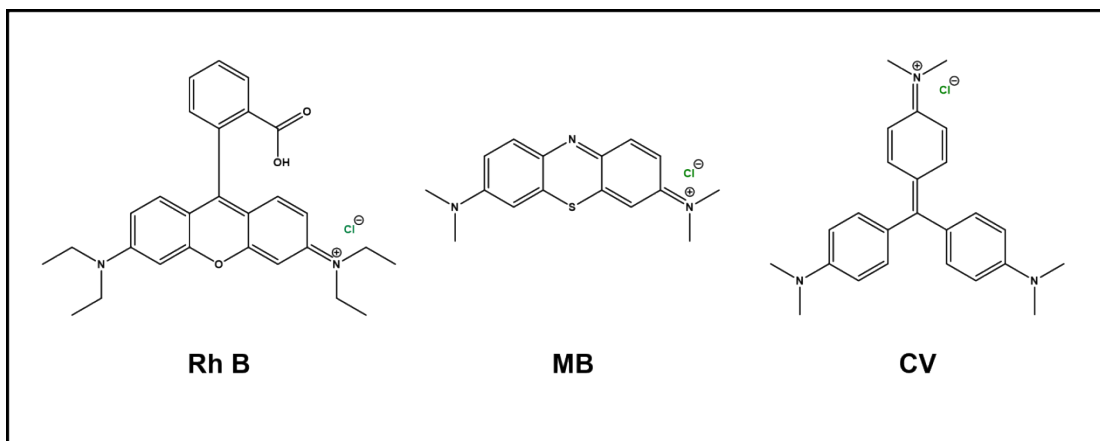


Fig. S8 Molecular structures of non-anionic organic dyes used in this work.

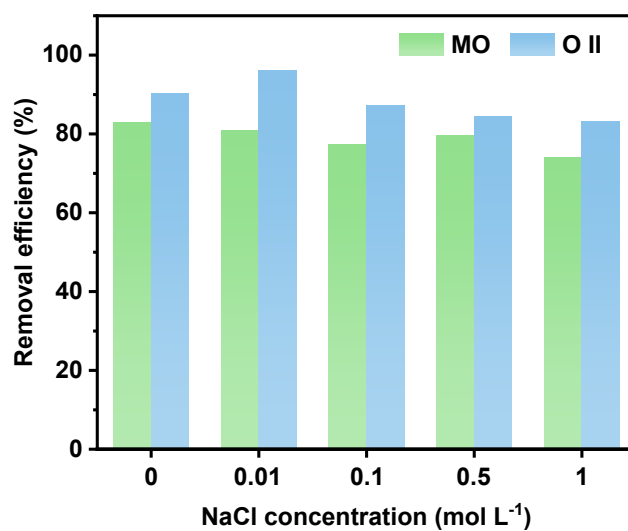


Fig. S9 Effect of ionic strength on the removal efficiency of S-iCOF for MO and O II ($C_0 = 30 \text{ mg L}^{-1}$) at 25 °C.

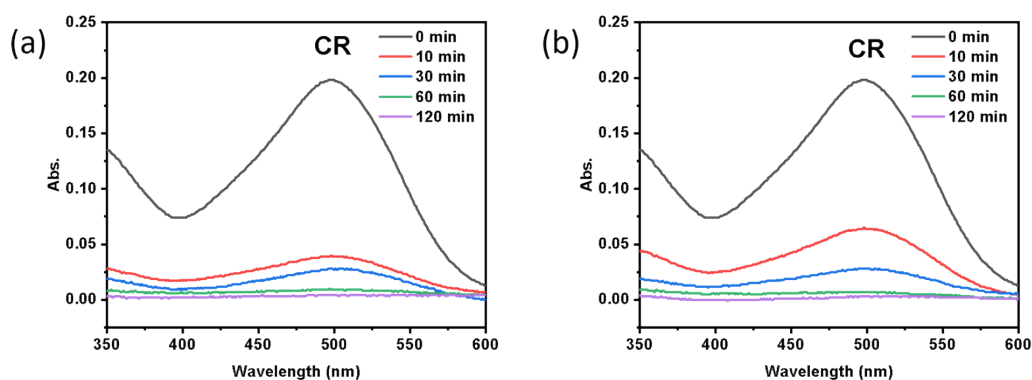


Fig. S10 UV/Vis absorption spectra of aqueous CR ($C_0 = 20 \text{ mg L}^{-1}$) Stirred treatment with (a) S-iCOF and (b) L-iCOF at the given times at $25 \text{ }^\circ\text{C}$.

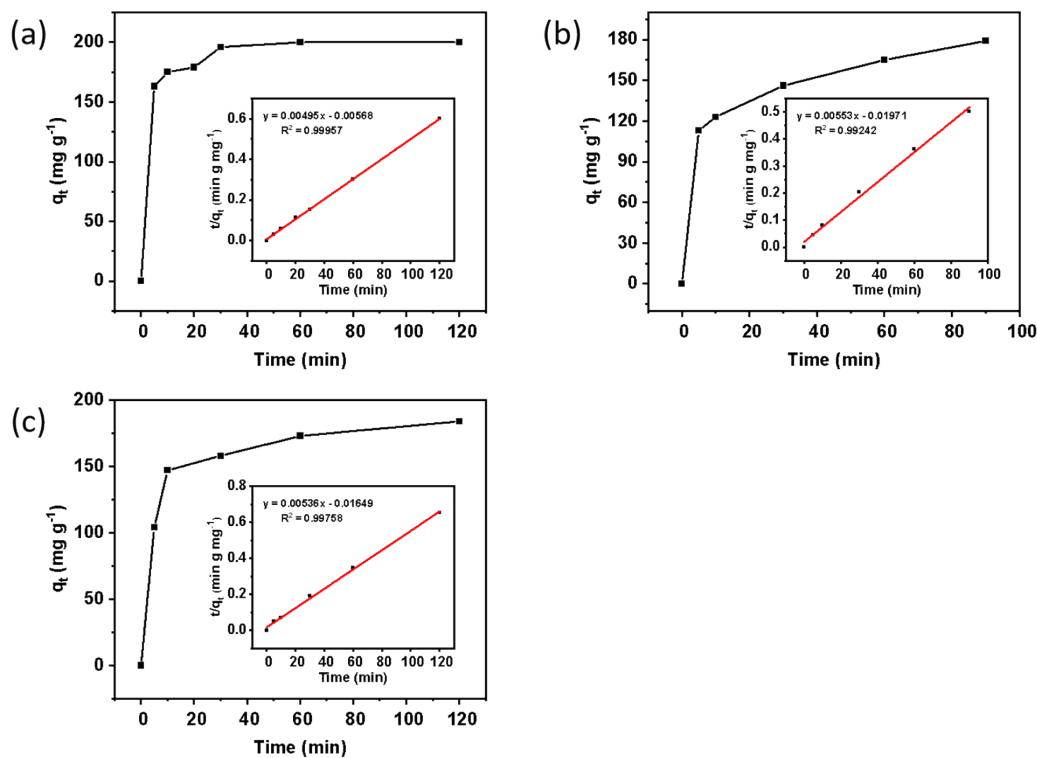


Fig. S11 Adsorption kinetics of L-iCOF toward aqueous (a) MO ($C_0 = 20 \text{ mg L}^{-1}$), (b) O II ($C_0 = 20 \text{ mg L}^{-1}$) and (c) OG 17 ($C_0 = 20 \text{ mg L}^{-1}$) solutions at $25 \text{ }^\circ\text{C}$. The insets show the pseudo-second-order kinetic plots of corresponding dye.

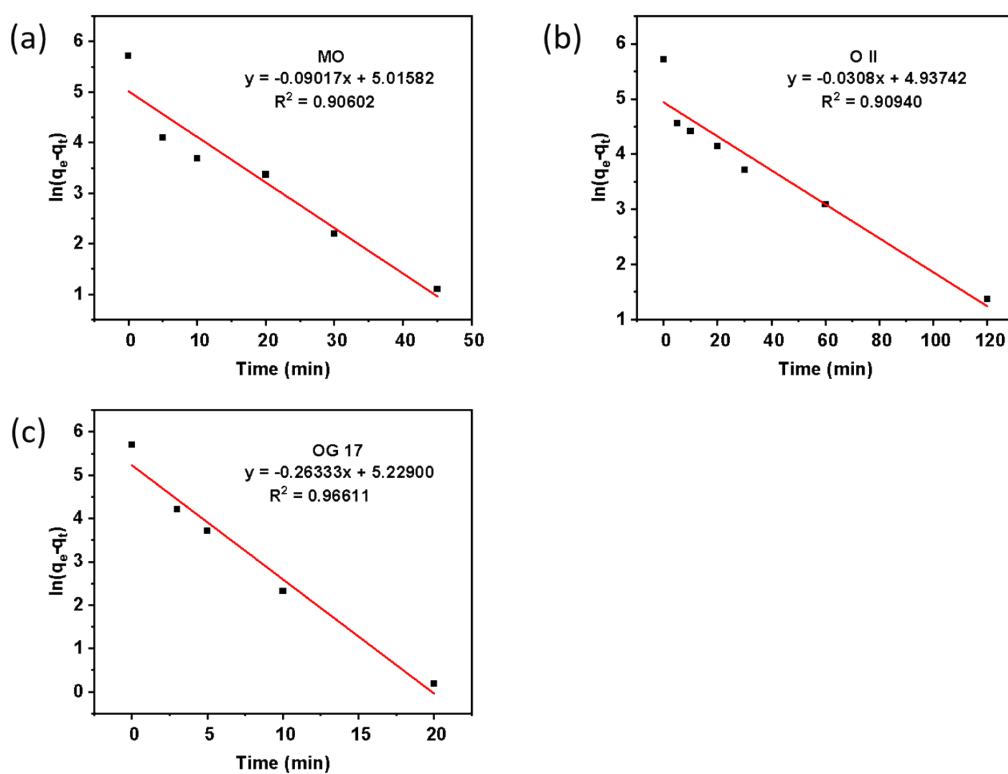


Fig. S12 Plots of pseudo-first-order kinetic on S-iCOF toward aqueous (a) MO ($C_0 = 30 \text{ mg L}^{-1}$), (b) O II ($C_0 = 30 \text{ mg L}^{-1}$) and (c) OG 17 ($C_0 = 30 \text{ mg L}^{-1}$) solutions at 25 °C.

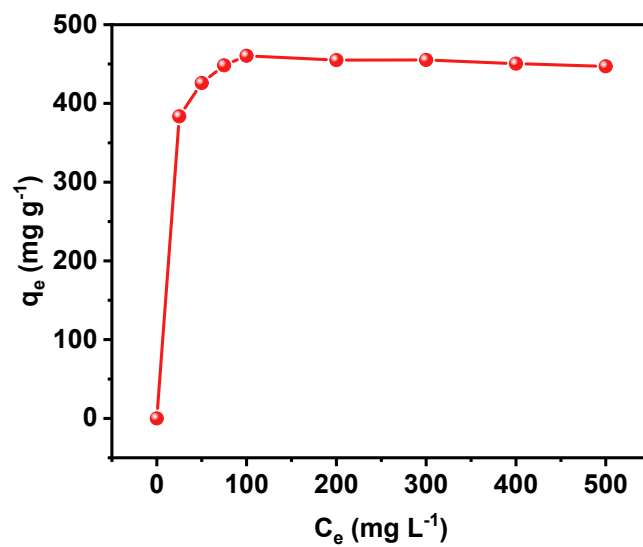


Fig. S13 Adsorption isotherms of S-iCOF for O II.

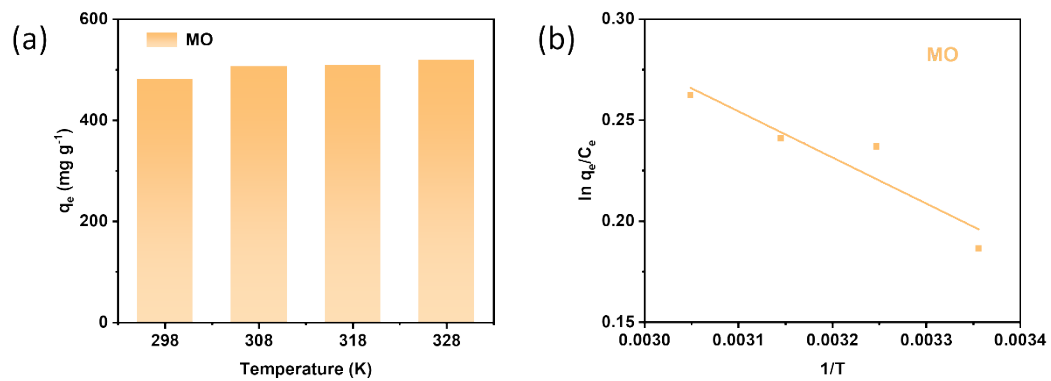


Fig. S14 (a) Adsorption capacities of S-iCOF toward MO ($C_0 = 400 \text{ mg L}^{-1}$) at different temperatures for 72 h. (b) Plots of $\ln q_e/C_e$ against $1/T$ for the adsorption of MO on S-iCOF.

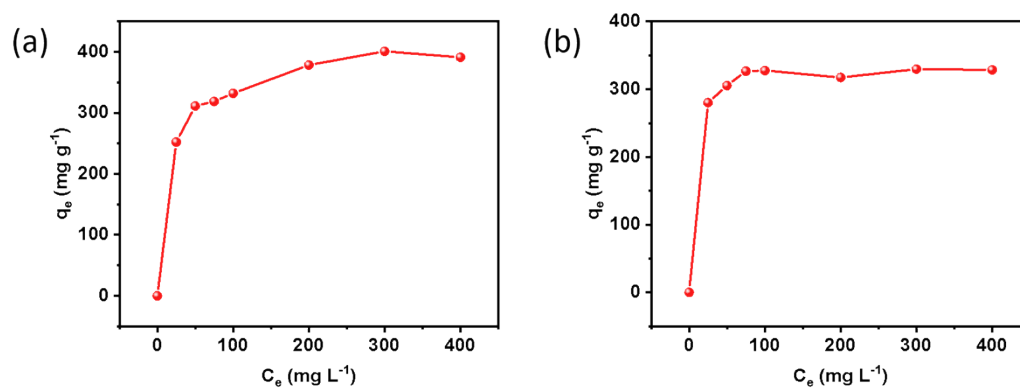


Fig. S15 Adsorption isotherms of L-iCOF for (a) MO and (b) O II.

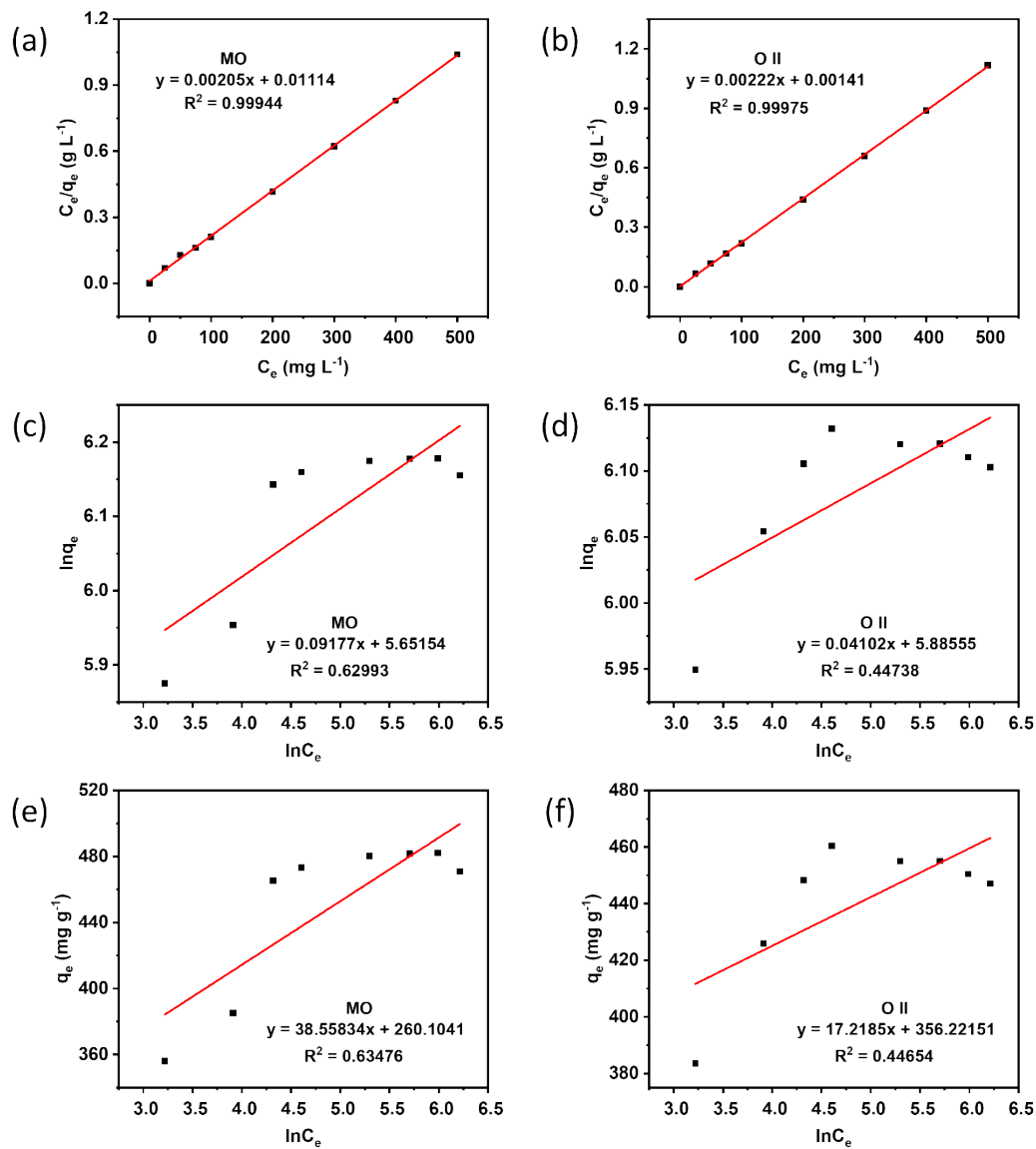


Fig. S16 Plots of the fitting of MO adsorption experimental data with (a) Langmuir, (c) Freundlich and (e) Temkin isotherm modes, also O II adsorption experimental data with (b) Langmuir, (d) Freundlich and (f) Temkin isotherm modes.

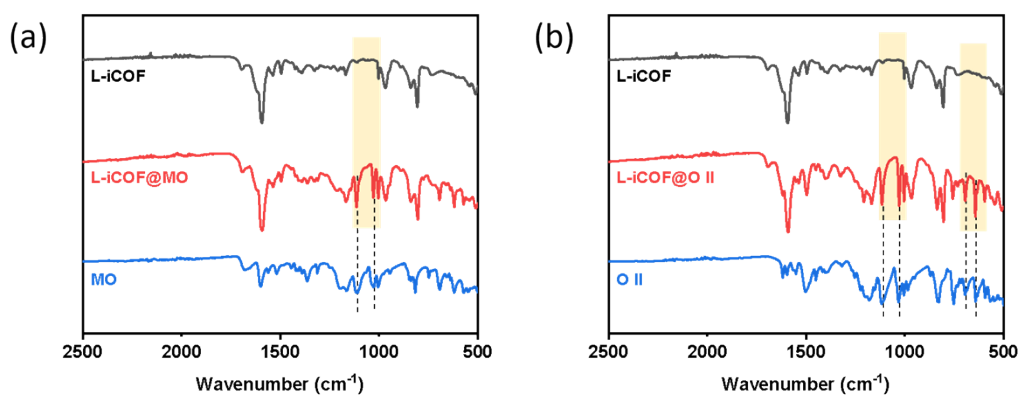


Fig. S17 FTIR spectra of L-iCOF before and after adsorption with MO (a) and O II (b) and the dye itself.

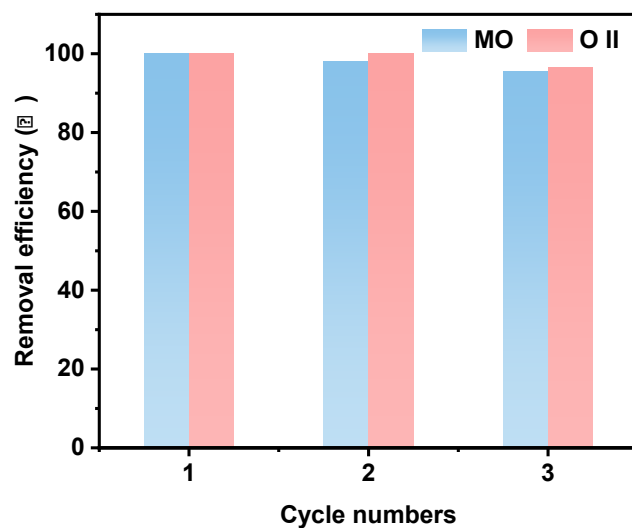


Fig. S18 Recyclability of L-iCOF in MO ($C_0 = 30 \text{ mg L}^{-1}$) and O II ($C_0 = 30 \text{ mg L}^{-1}$) aqueous solution.

Table S1 The equilibrium capacities, rate constant and correlation coefficient R^2 of dyes adsorption on S-iCOF.

Dye		MO	OG 17	O II
$q_{e,exp}$ (mg g ⁻¹)		364.32	349.63	381.5
Pseudo-first-order	$q_{e,cal}$ (mg g ⁻¹)	150.78	186.61	139.41
	k_1 (min ⁻¹)	0.09017	0.26333	0.03080
	R^2	0.90602	0.96611	0.90940
Pseudo-second-order	$q_{e,cal}$ (mg g ⁻¹)	303.03	301.20	303.95
	k_2 (g mg ⁻¹ min ⁻¹)	0.00309	0.00889	0.001
	R^2	0.99975	0.99994	0.99794

Table S2 The thermodynamic parameters for the adsorption of MO on S-iCOF.

Dyes	ΔH (kJ mol ⁻¹)	ΔS (J mol ⁻¹ k ⁻¹)	ΔG (kJ mol ⁻¹)			
			298 K	308 K	318 K	328 K
MO	1.90	7.99	-0.48	-0.56	-0.64	-0.72

Table S3 Comparison of adsorbents in this study with reported similar adsorbents towards MO.

Adsorbent	Adsorption capacity (MO, mg g ⁻¹)	Ref.
NH ₂ -MIL-88(Fe)/COF	106	<i>Inorganic Chemistry Communications</i> 172 (2025) 113475
TAPT-HMIPA-COF	185	<i>Journal of Hazardous Materials</i> 476 (2024) 135075
MA-BA COF	226	<i>Journal of Environmental Chemical Engineering</i> 11 (2023) 109890
Benzodiimidazole-COF	256	<i>European Polymer Journal</i> 133 (2020) 109764
ICOF	290	<i>RSC Advances</i> (2023) Issue 34
BiPy-MCOF	421	<i>Environmental Science and Pollution Research</i> 30 (2023) 34669
CEIL-S-KCC-1	507	<i>Journal of Colloid and Interface Science</i> 679 (2025) 555
L-iCOF	401	This study
S-iCOF	482	This study

Table S4 Comparison of adsorbents in this study with reported similar adsorbents towards O II.

Adsorbent	Adsorption capacity (O II, mg g ⁻¹)	Ref.
MC3	201	<i>Journal of Hazardous Materials</i> 424 (2022) 127401
Al13-Mt/C	250	<i>Applied Clay Science</i> 99 (2014) 229
VA-GNR	265	<i>Carbon Letters</i> 30 (2020) 123
AC-2	389	<i>Journal of Cleaner Production</i> 168 (2017) 22
Zr(IV)-CS-PT	476	<i>International Journal of Biological Macromolecules</i> 118 (2018) 340
L-iCOF	329	This study
S-iCOF	460	This study